UNCLASSIFIED

SECURITY CLASSIFICATION OF THIS PAGE (When Data Entered)

REPORT DOCUMENTATION PAGE

READ INSTRUCTIONS BEFORE COMPLETING FORM

1. REPORT NUMBER: TWENTY-SIX	2. GOVT ACCESSION NO.: AD-A088211
3. RECIPIENT'S CATALOG NUMBER:	
4. TITLE (and Subtitle): A Linear Response Theory Approach to Time-Resolved Fluorimetry	5. TYPE OF REPORT & PERIOD COVERED: Interim Technical Report,
6. PERFORMING ORG. REPORT NUMBER: 33	
7. AUTHOR(s): G. M. Hieftje and E. E. Vogelstein	8. CONTRACT OR GRANT NUMBER(s): N-14-76-C-0838
9. PERFORMING ORGANIZATION NAME AND ADDRESS: Department of Chemistry, Indiana University, Bloomington, Indiana 47405	10. PROGRAM ELEMENT, PROJECT, TASK AREA & WORK UNIT NUMBERS: NR -51-622
11. CONTROLLING OFFICE NAME AND ADDRESS: Office of Naval Research, Washington, D.C.	12. REPORT DATE: July 18, 1980
	13. NUMBER OF PAGES: 48
14. MONITORING AGENCY NAME & ADDRESS (if different from Controlling Office)	15. SECURITY CLASS. (of this report): UNCLASSIFIED
	15a. DECLASSIFICATION/DOWNGRADING SCHEDULE

16. DISTRIBUTION STATEMENT (of this Report)

Approved for public release; distribution unlimited.

17. DISTRIBUTION STATEMENT (of the abstract entered in Block 20, if different from Report)

DTIC ELECTE AUG 25 1980 S A

18. SUPPLEMENTARY NOTES

Prepared for publication in "Modern Fluorescence Spectroscopy", vol. 3, E. L. Wehry, ed., Plenum Press, Inc.

19. KEY WORDS (Continue on reverse side if necessary and identify by block number)

20. ABSTRACT (Continue on reverse side if necessary and identify by block number)

A new conceptual and instrumental approach to time-resolved chemical measurements is presented. Based on the concepts of information and linear response theory, the new approach is applicable to a number of different areas, including nuclear magnetic resonance spectrometry, high-speed kinetic measurements, gas chromatographic analysis, and time-resolved luminescence spectrometry. In the particular examples given, the new approach is applied to the determination of luminescence lifetime. Accuracy and simplicity of the method are emphasized and its application to chemical analysis discussed.

DD FORM 1 JAN 73 1473 EDITION OF 1 NOV 65 IS OBSOLETE S/N 0102-014-6601

UNCLASSIFIED

SECURITY CLASSIFICATION OF THIS PAGE (When Data Entered)

OFFICE OF NAVAL RESEARCH

Contract N14-76-C-0838

Task No. NR 051-622

TECHNICAL REPORT NO. 26

A LINEAR RESPONSE THEORY APPROACH TO TIME-RESOLVED FLUORIMETRY

by

G. M. Hieftje and E. E. Vogelstein

Prepared for Publication

in

"MODERN FLUORESCENCE SPECTROSCOPY",
vol. 3, E. L. Wehry, ed., Plenum Press, Inc.

Indiana University

Department of Chemistry

Bloomington, Indiana 47405

July 18, 1980

INTRODUCTION

The phenomenon of fluorescence has been recognized since the mid-nineteenth century, when it was first correctly described by Sir George Stokes (1). Even the measurement of fluorescence lifetimes was successfully approached as early as 1926 by E. Gaviola (2). However, only quite recently has instrumentation become available to permit the development of fluorimetry into a useful chemical tool. In particular, the development of practical techniques for time-resolved fluorescence measurements only became possible after about 1950, when radiation detectors and signal processing electronics with high sensitivity and nanosecond time resolution became commercially available. Since then, there has been a tremendous amount of activity in this field. Not only have several methods for the measurement of fluorescence lifetimes been well developed, but they have already been applied to many interesting problems in several areas of chemistry.

In this chapter, the measurement of luminescence lifetimes is treated from an unusual vantage point, specifically that of linear response theory. It will be shown how linear response theory can be employed to relate essentially all commonly used methods for time-resolved fluorimetry. Perhaps more importantly, it will be demonstrated that new approaches to sub-nanosecond lifetime measurement can be derived from information theory concepts. No attempt will be made to be exhaustive in the coverage of time-resolved measurement techniques, nor will an exhaustive review of the literature be provided. Rather, the goal of the chapter will be to provide a framework within which essentially all lifetime measurement techniques can be unified. To

begin, let us briefly examine the nature of time-resolved fluorimetry and learn how it can be viewed from the standpoint of linear response theory.

BASICS OF TIME-RESOLVED FLUORIMETRY

Fluorescence is a linear process (i.e. is proportional to the power of exciting radiation), and a unified understanding of the techniques for the measurement of fluorescence lifetimes can be obtained by viewing time-resolved fluorimetry from the standpoint of linear response theory. Therefore, let us digress a bit to introduce the basic concepts of linear response theory.

Linear Response Theory

In linear response theory, any system is described by specifying its transfer function. The transfer function completely describes the system's response to any time-dependent perturbation. These basic ideas are illustrated schematically in Figure 1. Clearly, the transfer function is itself an important system property. Moreover, various other system parameters can be determined from it.

There are two ways of specifying the transfer function of a system or network: by its frequency response function or by its impulse response function. The frequency response function gives the attenuation and phase shift caused by the system as a function of frequency. It can be measured by applying a sinusoidal perturbation to the system's input and measuring at the system's output the relative amplitude and phase of the resulting sinusoidal response. A plot of this amplitude and phase behavior as a function of frequency then constitutes the frequency response function. A schematic illustration of the determination of a

frequency response function is shown in Figure 2. Amplitude and phase fluorimetry are techniques which rely upon the frequency response function, as discussed later.

The impulse response function, on the other hand, gives the time response of the system to a delta function (impulse) perturbation. An ideal delta function can be thought of as an infinitely narrow spike of infinite amplitude. Consequently, an approximation to the impulse response function can be measured by applying a short duration pulse of large amplitude to a system's input and monitoring the resulting time response at the system's output. Figure 3 schematically illustrates such a measurement. Notice that the impulse response is a function of time, unlike the frequency response. As we shall see, these two functions are mathematically related. Understandably, the impulse response function is related to the pulse techniques for measuring luminescence lifetimes.

According to Fourier theory, an ideal impulse contains all frequencies. Therefore, applying a delta function input to a system is equivalent to simultaneously sending all frequencies into it. The impulse response function must then also contain all frequencies superimposed on each other, but each frequency component will have been attenuated and phase shifted according to the system's frequency response. Therefore, the impulse response function contains exactly the same information as the frequency response function. In fact, the two functions are entirely equivalent and can be simply related by Fourier transformation. Accordingly, if a system's impulse response function is known, its frequency components can be unscrambled by Fourier transformation to yield the frequency response function. Similarly, the impulse response function can be calculated from the frequency response function by inverse Fourier transformation.

Either the frequency or impulse response function completely determines the response of a system or device to any arbitrary input. In terms of the

frequency response function, the frequency spectrum of a system's output is related to that of the corresponding input signal by:

$$Y(f) = X(f)A(f) \tag{1-a}$$

$$\beta(f) = \alpha(f) + \phi(f) \tag{1-b}$$

In these equations, $Y(f)$ and $\beta(f)$ are the amplitude and phase portions of the output frequency spectrum, $X(f)$ and $\alpha(f)$ are similarly the components of the input signal's frequency spectrum, and $A(f)$ and $\phi(f)$ are the amplitude and phase of the system's frequency response function. In words, Equation (1-a) says that the amplitude of any frequency component in the output signal is equal to its amplitude in the input signal multiplied by the system's transmission at that frequency. Similarly, the phase of each frequency component in the output is just equal to its phase in the input plus the characgeristic phase shift of the system at that frequency. These relations make sense intuitively; moreover, they are quite familiar for electronic systems, such as RC filter circuits and amplifiers.

In terms of the impulse response function, on the other hand, the response of a system, $R(t)$, to an input perturbation, $P(t)$, is given by the convolution of the input perturbation with the system's impulse response function, $I(t)$. This convolution process is described mathematically by the relation:

$$R(t) = P(t) * I(t) = \int_0^t P(T)I(t-\tau)dT \tag{2}$$

where the asterisk denotes convolution, t is time, and τ is just a dummy integration variable. A simple explanation of the form of the convolution integral

is possible if one analyzes more closely the convolution process itself.

Convolution. Let us intuitively derive the mathematical expression for convo ion by considering a series of experiments with some hypothetical test system; Figure 4 illustrates this approach schematically. In each experiment the system is perturbed with a specific input signal, P(t), and we try to describe mathematically what the system's response, R(t), will be in each case.

1) The system is perturbed at time t = 0 with a delta function input of amplitude P(0). The response of the system after time t = 0 will be, by definition, the system's impulse response function, I(t) scaled in amplitude by that of the perturbing impulse. This experiment is illustrated schematically in Figure 4(a), and is described mathematically by

$$P_1(t) = P(0)\delta(t) \tag{3-a}$$

$$R_1(t) = P(0)I(t) \tag{3-b}$$

2) The system is perturbed with a delta function input of amplitude $P_1(t)$ at time t = T. The response of the system will again be just the impulse response scaled by the amplitude of the input pulse; however, the response is now displaced in time to t = T. Figure 4(b) schematically illustrates this experiment, and its mathematical description is

$$P_2(t) = P_1(T)\delta(t - T) \tag{4-a}$$

$$R_2(t) = P_1(T)I(t - T) \tag{4-b}$$

3) The system is perturbed with a train of delta-function pulses. Specifically, let the system be perturbed by the following series of impulses: a delta function of amplitude $P(0)$ at time $t = 0$, a delta function of amplitude $P(T_1)$, as time $t = T_1$, a delta function of amplitude $P(T_2)$ at time $t = T_2$, etc. From the preceding discussion, each of these input impulses induces a response from the system in the form of the system's impulse response function, scaled by the amplitude of the input pulse and displaced in time by the pulse's time of occurrence. The total response of the system to the train of perturbing impulses is then just the sum of the contributions from all of the impulses; i.e. the amplitude of the system's output at any time t will be equal to the sum of the amplitudes at that time of the responses induced by all preceding input impulses. This experiment is illustrated schematically in Figure 4(c), and it is described mathematically by

$$P_3(t) = P(0)\delta(t) + P(T_1)\delta(t - T_1) + P(T_2)\delta(t - T_2) + \ldots \qquad (5\text{-a})$$

$$R_3(t) = P(0)I(t) + P(T_1)I(t - T_1) + P(T_2)I(t - T_2) + \ldots + P(T_n)I(t - T_n) = \sum_{T=0}^{t} P(T)I(t - T) \qquad (5\text{-b})$$

where $T_n \leq t$, but $T_{n+1} > t$.

4) Finally, let us consider a perturbation of the system with some real signal of finite duration, whose amplitude-time profile is given by $P(t)$ [cf. Fig. 4(d)]. This input signal can be viewed as a train of delta function pulses, just like that of the preceding example but the interval between successive pulses has become infinitesimal and the amplitude of the pulses follows the shape of the function $P(t)$. Therefore, the response of the system

in this the general case is also described by Equation (5 b), with just one minor modification: the summation must be replaced by an integral, since successive pulses in the imiginary train of delta function pulses are now infinitely close in time. If this substitution is made, one does in fact arrive at the convolution integral given in Equation (2).

Practical Considerations

From the foregoing discussion, it should be apparent that either the impulse response or frequency response function can be employed to describe the temporal response characteristics of a system we wish to test, and that both methods provide the same information. However, depending on the particular experimental situation, one method or the other might be superior. Therefore, it is appropriate to briefly consider the experimental requirements for measuring each kind of function.

Obviously, to determine an impulse response function, the system under test must be perturbed with a source of energy which appears temporally as a spike. Ideally this spike or impulse should approach a mathematical delta function; that is, it should possess infinite amplitude and zero width and have an integral of unity. In practice, however, the perturbing source must emit a spike which is narrow with respect to the temporal characteristics of the transfer function being measured. Moreover, the maximum the amplitude of the spike will be limited practically by the linearity of the system being tested, while the minimum amplitude will be bounded by the sensitivity of the system to the perturbation and the required magnitude of the response which it elicits. Measurement of the elicited impulse response function simply requires a detector capable of monitoring the response and of following faithfully its temporal behavior.

Obviously, severe constraints exist in the choice of a real perturbation source for impulse response determinations. Often, the perturbing scurce is

not brief enough in duration, which results in a distorted response trace. Alternatively, the source might be too weak to evoke a measurable response or so intense that non-linear behavior is produced. As will be indicated later, all these limitations exist in time-resolved fluorimetry and great care must be taken to overcome or avoid them.

In the measurement of a frequency response function, several alternative approaches exist. The simplest such approach, and one which produces the highest signal-to-noise ratio, simply involves perturbing the system under test with a sinusoidally modulated energy source and observing the resulting response with a tuned, phase-sensitive detector. A linked frequency sweep of source and detector then provides both parts (phase and amplitude) of the frequency response function. Alternatively, several fixed-frequency sources can perturb the system simultaneously, with the resulting response being examined either by a series of individual frequency and phase-sensitive detectors or with a single frequency-swept device. This latter kind of device is termed a "spectrum analyzer." Of course, the second method for frequency response measurement results in measurements at only specific, discrete frequencies and limits the resolution of the resulting response curve.

To improve resolution on the curve, additional perturbing sources could be added, with an attendant increase in complexity. In the limit, one could envision an infinite number of discrete sources, to enable the entire spectrum to be resolved. Interestingly, this seemingly exotic limit is relatively simple to implement practically. White noise sources are available which emit energy over enormous frequency ranges (d.c. to GHz) and provide outputs which, for most purposes, appear to have originated from just such an infinite array of sources. Thus, with a white noise source, a system can be perturbed simultaneously over a broad frequency range, with the re-

sulting response being simply monitored by a swept-frequency spectrum analyzer.

Frequency response measurements, be they swept, multi-frequency, or noise input approaches, are often superior to impulse response measurements. Whereas the impulse requires all energy which elicits a measured response to be concentrated in a single instant, the perturbing energy can be spread out in time when the frequency domain is employed. This capability often results in greater detectability, signal-to-noise ratios, and less danger from saturation (non-linearity) than is found in the pulse techniques. As a result of this limitation, engineers employing linear response theory have devised a simple way of obtaining impulse response functions using multi-frequency or white noise perturbing sources. The basic idea behind these measurements is outlined in Figure 5.

As shown in Figure 5A, there is a fixed mathematical relationship between white noise and a delta function. Specifically, the delta function is obtained by autocorrelating the noise. That this result arises can be appreciated from the basic nature of the correlation process (3). In particular, the process of autocorrelation produces a phase registration of all of the frequency components in any complex (non-sinusoidal) wave form. That is, each frequency component in the wave form is converted to a cosine wave and therefore has its maximum value at a location equal to zero on the horizontal axis. Consequently all frequency components in the complex wave form align at this phase-related point, causing their amplitudes to add. At all other points on the horizontal axis, however, the different frequency components in the original waveform will be out of phase by varying degrees and, when summed, will produce a resultant which is probably lower than the amplitude of the "zero" point. For a wave form like white noise, which contains all frequencies, there will be an

infinite number of such waves, so that for every one which has a large positive value at some horizontal axis location, there will be another which has an equal but negative amplitude, causing the resultant to be zero. Consequently, for a completely random wave form such as white noise, all frequency components add only at the "zero" point and produce everywhere else a value of zero.

How these concepts can be applied to the measurement of an impulse response function is illustrated in Figure 5B. In this case, white noise is not correlated with itself (autocorrelation), but rather is correlated with a version of itself which has been passed through the device we wish to test. Intuitively, one would imagine that the random waveform would be altered upon passing through this device; in particular, that some of its frequency components would have been attenuated or phase-shifted somewhat, in accordance with the system's frequency response function. For simplicity, let us assume here that this system attenuates the high-frequency components in the random waveform. As a consequence, one would expect these high-frequency components also to be absent from the cross-correlation function calculated between the two waves. Loss of these high-frequency components would strip the impulse response function of its rapidly changing features and would yield a smoothed waveform rather than the delta function which would otherwise have been produced. Although this discussion has centered on the transmission of a random waveform through a device to be tested, it should be clear that the same considerations apply to a response elicited by such a wave form.

This alternative scheme for the measurement of impulse response functions has several attractive features. Like the frequency response measurements, it applies the perturbation to the system under test over an extended time period, rather than all at once. The system is thus less likely to be strained or driven into non-linear response. In addition, this alternative method is relatively

immune to a constant offset in the input perturbation. This feature is a substantial advantage in some applications. For example, the impulse response function of a large electrically driven turbine can be obtained while the turbine is running, simply by adding a small random electrical variation to the constant drive current and by cross-correlating that random wave form with the minute fluctuations in the turbine's velocity which result. Finally, this method can prove advantageous just because of the ubiquitous nature of white noise or random processes. Recognizing that most things we examine are perturbed by the natural, often stochastic events in their environment, scientists have devised extremely clever ways to measure response functions without the need for external perturbation (4-7).

Many examples could be cited where impulse or frequency response functions are used in science. Because of the simplicity of their interpretation, the impulse techniques are the most widely employed. For example, Fourier transform nuclear magnetic resonance spectrometry is essentially an impulse technique, wherein a pulse of radiofrequency energy is used to elicit a response from nuclei (their free induction decay). Impulse methods are also used in perturbation techniques for the measurement of rapid kinetics. (e.g. pressure-jump and temperature-jump approaches). Finally, analytical gas and liquid chromatography are impulse-type measurements, and involve the application of a pulse of sample material, which yields as an impulse response function the desired chromatogram.

These examples hopefully reveal the importance and scope of impulse and frequency response measurements and also suggest that perturbing sources need not be electrical in nature but might consist of energy input in the form of a light pulse, a temperature variation, or an increment of chemical sample. Let us now turn our attention to an area in which these approaches become especially useful--time-resolved fluorimetry.

Linear Response Functions in Time-Resolved Fluorimetry

How can the concepts of linear response theory be applied to time-resolved fluorimetry? In such an application, the generalized system discussed in the preceding section is specifically the fluorescent sample under study. Applying a time-dependent perturbation correspondingly translates into illuminating the sample with a source whose output radiance varies as a function of time. Similarly, monitoring the response of the system to the perturbation now implies measuring the time-dependent intensity of the resulting fluorescence. Again, the response and the input perturbation are related via the system's impulse response (transfer) function. For a fluorescent sample, this transfer function is determined by the decay kinetics of the probed excited state.

The objectives of time-resolved fluorescence studies are the measurement of excited-state lifetimes and study of the decay kinetics of species in excited states. From the standpoint of linear response theory, an experiment in time-resolved fluorimetry involves measuring the transfer (impulse response) function of the molecular system being studied; from this function the excited-state lifetime or decay rate constant of interest can be calculated.

Because there are two ways of specifying a system's transfer function, there are two classical approaches to time-resolved fluorimetry. The pulse techniques for the measurement of fluorescence lifetimes (8-10) constitute one approach. With these techniques it is the impulse response function of the molecular system being studied that is measured. The other classical approach to time-resolved fluorimetry employs the measurement of points on the frequency response function of the fluorescent system. This approach includes the modulation and phase-shift (8,11,12) techniques for the measurement of fluorescence lifetimes. Finally, a group of new techniques has recently arisen which revolves around the use of a stochastic or noisy perturbation and either cross-correlation or

spectrum analysis to generate, respectively, the impulse response function or frequency response function of a fluorophore.

Let us now take a closer look at these appraoches to time-resolved fluorimetry. In particular, let us consider what the impulse and frequency response functions of a fluorescent sample look like and how they are related to the excited-state lifetime of the fluorophore. Also to be discussed are the experimental measurements involved and how lifetime values can be calculated from the data in each case. Finally, new methods based on correlation will be examined, and their capabilities compared with the classical schemes.

Pulse Fluorimetry

In the pulse techniques for the measurement of fluorescence lifetimes, the sample of interest is illuminated with an intense, brief pulse of light and the intensity of the resulting fluorescence is recorded as a function of time. If the exciting light pulse is sufficiently short, the measured fluorescence decay curve will be a good approximation to the sample's impulse response function.

In general, several processes contribute to the relaxation of molecules in solution from an excited singlet state: the radiative process of fluorescence as well as such nonradiative processes as internal conversion, intersystem crossing, and quenching by other species present in the solution. Fluorescence, internal conversion, and intersystem crossing are unimolecular processes; therefore they follow simple first-order kinetics. In addition, quenching by other species, although a bimolecular process, can in most cases be described in terms of pseudo-first-order kinetics. Therefore, for most fluorescent samples, the excited-state population established by an impulse of exciting light will decay

exponentially, according to the familiar decay law for first-order kinetics. The rate of this decay is determined by the sum of the rates of all contributing relaxation processes. Because the intensity of fluorescence from a sample reflects its excited-state population, it follows that the impulse response function of such a sample is just a simple decaying exponential; moreover, the decay constant of this function directly gives the overall relaxation rate for the probed excited state of the fluorophore.

To be more quantitative, for most fluorescent samples the impulse response function, I(t), will have the form:

$$I(t) = I_0 e^{-kt} \tag{6}$$

where I_0 is just a scaling factor representing the peak fluorescence intensity, and k represents the overall relaxation rate for the probed excited state. The value of k, in turn, is given by

$$k = k_F + k_{IC} + k_{IX} + k_Q \tag{7}$$

where k_F, k_{IC}, and k_{IX} are the first-order rate constants for fluorescence, internal conversion, and intersystem corssing from the probed state, respectively, and k_Q is the pseudo-first-order rate constant for bimolecular quenching of that state.

Often, the decay kinetics of an excited state are described in terms of its lifetime. The fluorescence lifetime of an excited state is by definition the time required for the excited state population to decay to 1/e, or ~37%, of its initial value, following excitation by an impulse of light. Therefore,

the lifetime, τ, is simply the time corresponding to the 1/e point of the fluorophore's impulse response function. From Equation (6) it follows that

$$\tau = 1/k \tag{8}$$

which indicates that the lifetime of an excited state gives the reciprocal of the state's overall decay rate constant.

Clearly, for any fluorescent sample which exhibits such exponential decay behavior, the lifetime of the probed excited state can easily be calculated from the sample's impulse response function, i.e. its experimental fluorescence decay curve. In practice, one can simply prepare a semi-logarithmic plot of the fluorescence decay data and determine the slope of the resulting straight line. Taking the logarithm of Equation (6), one obtains

$$\log I(t) = -kt + \log I_0 \tag{9}$$

which represents a straight line with slope k. This procedure constitutes the so-called graphical slope method for the evaluation of fluorescence lifetimes from pulse fluorimetric data.

Although most fluorescent samples exhibit the simple exponential decay behavior discussed above, there are some important exceptions. Specifically, any sample which contains more than one fluorescent species will exhibit non-exponential decay in pulse fluorimetry. For such a sample, the impulse response function is a sum of exponential terms, with one term for each fluorescent species present. In general, it then becomes difficult to extract valid excited-state lifetime values for the individual components from the sample's fluorescence decay function.

In addition, not always can bimolecular quenching be described in terms of pseudo-first-order kinetics. Therefore, some one-component fluorescent samples might also exhibit non-exponential decay behavior. Study of the form of the fluorescence decay function for such samples can, however, reveal much about the mechanism of the quenching process involved.

The relaxation rates for excited singlet states are often greater than 10^9 sec^{-1}; accordingly, fluorescence lifetimes fall in the nanosecond and subnanosecond time range. Therefore, the measurement of fluorescence lifetimes by pulse techniques poses some difficult instrumental problems; sources capable of generating nanosecond or subnanosecond light pulses are required, and sensitive detectors and signal processing electronics capable of responding on this time scale are needed. Significantly, many fluorophores have excited-state lifetimes which are of the same order or even shorter than the time-resolution capabilities of available instrumentation. If the duration of the light pulses provided by the excitation source is not negligible relative to the lfietime of the fluorophore being studied, the sample's measured fluorescence will not be an accurate representation of its impulse response function. Similarly, if the response of the detection system is limited in the time range of interest, then the measured fluorescence signal will be distorted. In such cases, the measured fluorescence decay curve will be the convolution of the excitation light pulse and the impulse response of the detection system with the desired impulse response function of the sample. Therefore, the determination of very short fluorescence lifetimes requires deconvolution analysis (13) in order to extract the true impulse response function of the sample from the experimentally measured fluorescence decay curve.

Modulation and Phase Fluorimetry

Let us now consider what the frequency response function of a fluorescent

sample looks like. Recall from the earlier discussion that a system's impulse and frequency response functions can be simply related by Fourier transformation. Therefore, for any fluorescent sample that exhibits simple exponential decay behavior in pulse fluorimetry, the frequency response function is just a Lorentzian, i.e., the Fourier transform of an exponential. The amplitude, A(f), and phase, $\phi(f)$, of a Lorentzian obtained by Fourier transformation of an exponential with decay time τ, are given by

$$A(f) = \frac{1}{(1 + 4\pi^2 f^2 \tau^2)^{\frac{1}{2}}} \tag{10-a}$$

$$\phi(f) = \arctan(2\pi f \tau) \tag{10-b}$$

The relationship of a fluorophore's frequency response function to its excited-state lifetime, τ, can be expressed in terms of the frequency at the half-maximum point of either the amplitude or phase position of the frequency response function. From equations (10-a) and (10-b) one obtains the following relations:

$$\tau = \frac{\sqrt{3}}{2\pi} \cdot \frac{1}{f_{\frac{1}{2}}} \tag{11-a}$$

$$\tau = \frac{1}{2\pi} \cdot \frac{1}{f_{45^\circ}} \tag{11-b}$$

where $f_{\frac{1}{2}}$ denotes the frequency at the half-maximum point of the amplitude response function [i.e. the frequency at which $A(f) = \frac{1}{2}$], and f_{45° is the frequency at the half-maximum point of the phase portion of the frequency response function [i.e. the frequency at which $\phi(f) = 45^\circ$]. Notice that τ is simply the reciprocal of either $f_{\frac{1}{2}}$ or f_{45° times a constant. A Lorentzian frequency response function and its relationship to the excited-state lifetime of the corresponding fluoro-

phore are illustrated in Figure 6.

In the conventional modulation and phase-shift techniques for the measurement of fluorescence lifetimes, the sample of interest is illuminated with a source whose output is sinusoidally modulated at some frequency. The resulting fluorescence is observed and will also be sinusoidally modulated as the source frequency. In the modulation techniques, the modulation depth of the fluorescence relative to the exciting light is determined. In the phase-shift techniques, on the other hand, the phase shift of the modulated fluorescence relative to the exciting light is measured. From the standpoint of linear response theory, these techniques simply involve the determination of single points on the frequency response function of the sample. In either case, the excited-state lifetime of the fluorophore can easily be calculated from the experimental data.

Modulation fluorimetry involves the measurement of one point on the sample's amplitude response function, namely the value of A(f) at the particular modulation frequency used in the experiment. Therefore, solution of Equation (10-a) yields the expression

$$\tau = \frac{1}{2\pi f_0} \left(\frac{1}{A_0^2} - 1\right)^{\frac{1}{2}} \qquad (12\text{-a})$$

for the excited-state lifetime of the fluorophore, where A_0 is the measured relative modulation depth of the fluorescence and f_0 is the modulation frequency. In phase fluorimetry, on the other hand, the value of $\phi(f)$ is measured at the modulation frequency of the experiment, i.e. one point on the phase portion of the sample's frequency response function is determined. In this case, τ can be calculated from the measured phase shift, ϕ_0, between the modulated fluorescence and the exciting light from Equation (10-b), viz.,

$$\tau = \frac{1}{2\pi f_0} \tan \phi_0 \qquad (12\text{-b})$$

where f_0 again represents the particular modulation frequency used in the experiment.

Note that the Lorentzian frequency response illustrated in Figure 6 agrees well with our intuitive feeling for how a fluorophore should repond to modulated exciting light. At low modulation frequencies we would expect the excited-state population in the sample, and therefore the intensity of sample fluorescence, to closely follow the variations in exciting light. Thus, there should be little attenuation or phase shift of the modulated fluorescence compared to the exciting light. This behavior is reflected in the Lorentzian frequency response function by amplitude values near unity and phase values near zero at low frequencies. In contrast, at higher modulation frequencies we would expect the excited-state population in the sample to no longer follow faithfully the variations in exciting light, because of the finite lifetime of the excited state. This behavior is seen as a phase lag and decreased modulation depth in the observed fluorescence. Accordingly, the phase of the Lorentzian frequency response function increases from 0° toward 90°, and its amplitude decreases from 1 toward 0 as frequency increases. Furthermore, we would expect that a fluorophore with a short excited-state lifetime could follow closely higher modulation frequencies than a fluorophore with a longer excited-state lifetime. In fact (as stated earlier), the frequencies at the half-maximum points of the amplitude and phase spectra (cf. Fig. 6) are inversely proportional to the excited-state lifetime of the fluorophore.

Because fluorescence lifetimes are ordinarily very short, high modulation frequencies are required to provide a measurable phase shift or attentuation in

the detected fluorescence signal. Accordingly, the measurement of fluorescence lifetimes by modulation and phase-shift techniques can best be accomplished with light modulated in the megahertz to gigahertz frequency range. Therefore, this approach to the measurement of fluorescence lifetimes, like the pulse method, requires sophisticated instrumentation.

As indicated earlier, a phase-shift or amplitude measurement at a particular modulation frequency corresponds to the determination of just one point on the frequency response function of the fluorescent sample. In theory, the whole response function of the sample could be determined by repeating these measurements over a broad range of modulation frequencies. In practice, however, the difficulties associated with light modulation at frequencies in the megahertz-gigahertz range have limited conventional modulation and phase fluorimeters to the use of only one, two, or three discrete modulation frequencies. If the sample of interest is known to exhibit simple exponential decay behavior, this limitation is not serious. However, non-exponential decay behavior, i.e. deviation of the frequency response function from the Lorentzian form, is not detectable from a single phase or amplitude measurement. If measurements are made at two or three modulation frequencies, deviation from Lorentzian frequency response character is still defined by only two or three data points. Therefore, study of the decay kinetics of samples which exhibit non-exponential decay behavior is difficult with conventional phase or modulation fluorimeters. Recently, a modulation fluorimeter has been constructed based on a CW laser as a multifrequency-modulated source (14,15). This instrument should be applicable to the study of complex fluorescence decay behavior, for it enables amplitude measurements to be made at a large number of frequencies, thus accurately defining the sample's entire frequency response function.

Although pulse fluorimetry is better suited for the study of complex decay behavior than are modulation or phase fluorimetry, these latter techniques possess advantages in the measurement of very short fluorescence lifetimes. Because the determination of such short lifetimes requires the use of extremely high modulation frequencies, the modulation of the measured fluorescence signal is usually distorted by the limited frequency response of the detection system being used. Conveniently, correction for the response characteristics of the detection system is straightforward in modulation and phase fluorimetry. In the frequency domain (unlike in the time domain), "deconvolution" involves a simple division [in modulation fluorimetry, cf. Eq. (1-a)] or subtraction [in phase fluorimetry, cf. Eq. (1-b)]. In contrast, pulse fluorimetry requires correction for instrument characteristics by actual deconvolution analysis [cf. Equation (2)].

Correlation-Based Methods in Time-Resolved Fluorimetry

As indicated earlier, either the impulse or frequency response functions can be generated through use of a randomly varying perturbation source. If the impulse response function is desired, the source's fluctuations must be cross-correlated with the elicited response; if the frequency response is desired, it is only necessary to employ a swept frequency analyzer. Let us now examine how these concepts can be applied to the measurement of luminescence lifetimes.

Figure 7 illustrates schematically the kind of instrumentation which would be required to obtain a luminescence lifetime using the correlation approach. As before, the system being perturbed is the fluorescent species under study; its perturbation is a time-varying light flux and its observed response to this perturbation is the observed luminescence. However, in the present case,

the light flux is randomly modulated either internally or by means of an external modulator as shown. Excitation and emission monochromators isolate the wavelengths of interest and a high-speed photodetector converts the fluctuating luminescence to a proportional current for processing. This processing involves either the measurement of a frequency response function by means of a spectrum analyzer or an impulse response (decay curve) with a cross-correlation computer.

Unfortunately, the hypothetical instrument in Figure 7 cannot be simply implemented in the laboratory. For the displayed impulse or frequency response function to accurately reflect the kinetics (time dependence) of the fluorophore under investigation, the correlation computer must be capable of displaying subnanosecond-level data, the spectrum analyzer must be able to register frequencies in the GHz regime, and the light source must be randomly modulated over a frequency range from dc to several GHz. If these conditions are not met, extensive deconvolution procedures will be necessary and the resulting calculated decay kinetics will be less precise. Let us then examine the kinds of devices which might be realistically employed for, respectively, the source, spectrum analyzer, and correlation computer.

For the source, what is needed is a device whose emitted flux varies randomly over a broad frequency range. Obviously, the simplest such device is a CW lamp. Although we ordinarily consider such a lamp to be just a source of dc light, its beam is actually comprised of a photon flux; the random nature of photon emission and detection produces in the source emission a white noise character. Unfortunately, this noisy component is a relatively small fraction of the dc level of the source and the dc level contributes strongly to the shot noise produced upon detection of the beam. Consequently, calculations show that a luminescence decay curve obtained through use of this source in a cross-correlation scheme would exhibit at best a signal-to-noise ratio of 1, hardly

a desirable situation.

To generate higher signal-to-noise ratios, what is needed is a source whose amplitude is modulated at a greater depth than that of a CW lamp. Included in such sources might be free-running or randomly driven flash lamps, electro-optically or acousto-optically modulated CW light sources, and CW lasers. This latter source deserves further comment and is the one most often employed in this cross-correlation approach.

Noise in a CW laser arises not only from the random generation and arrival of photons, but from a phenomenon termed "mode noise." Mode noise originates in a laser's spectral structure and results from beating of individual modes with each other. It will be recalled that modes in a laser are separated by c/2L, where c is the speed of light and L is the laser's cavity length (the distance between the laser's mirrors). These modes will extend over the entire emission bandwidth of the lasing medium; for an argon-ion laser this range is approximately 4 GHz whereas for a dye laser it can be larger than 200 GHz. Beating of these modes with each other then produces a series of frequencies, spaced by c/2L, at which the laser is simultaneously modulated. Moreover, these discrete frequencies will extend as high as the emission bandwidth of the lasing medium (i.e. 4 GHz for an argon-ion laser). Thus, for a 1 meter argon-ion laser, c/2L will be 150 MHz, and the laser will appear to be amplitude modulated at all discrete frequencies from 150 MHz to approximately 4 GHz in increments of 150 MHz. The laser will therefore not be a truly random source, but its output will appear to be random and will in fact be modulated over a sufficiently broad frequency range.

The use of laser mode noise in a frequency response function approach to determining luminescence lifetimes was recently described (14,15); a schematic diagram

of the instrument is shown in Figure 8. In this work, a CW laser served as a multi-frequency modulated source and a spectrum analyzer was employed to display the frequency response function of several fluorophores which were investigated. From Figure 8, one can derive an intuitive feeling for how this scheme works. The top spectrum on the right side of Figure 8 displays the spectrum analyzer output which would be expected if the sampled cell contained simply a scattering medium. In such a case, the spectrum would indicate the amplitude of fluctuations in the laser's output. As described above, these fluctuations extend to extremely high frequencies and are present at discrete intervals. In contrast, the bottom spectrum in Figure 8 indicates the spectrum analyzer output when the scattering medium is replaced by a fluorophore capable of being excited by the fluctuating laser radiation. To understand this spectrum, recall that the laser is, in essence, self-amplitude modulated at each of the discrete frequencies indicated in the upper spectrum. Obviously, the excited state of the fluorophore can follow the slowest of these fluctuations quite faithfully and accordingly will yield a strong amplitude modulation in fluorescence at those frequencies. However, the finite exited-state lifetime of the fluorophore prevents it from fluctuating at the highest laser beat frequencies, to produce a gradual roll-off. As described in the section on linear response theory, this roll-off should follow a Lorentzian pattern, betraying the exponential exited-state decay behavior.

In reality, displayed spectra are never as clean as those shown schematically in Figure 8. Real plots, reproduced in Figure 9, reveal that the discrete flucutations in laser radiation are not all equal in amplitude, requiring the beat-frequency spectra from fluorophores to be normalized by the amplitudes of individual beat frequencies. Thus, the two right-hand spectra in Figure 9 would

be divided by that shown in Figure 9A. As suggested earlier, this division is especially meaningful here, since data are displayed in the frequency domain. Therefore, this normalization actually constitutes deconvolution.

Normalization of the spectra in Figure 9 results in the frequency response curves shown in Figure 10. As illustrated, the resulting data points (open circles) for the two fluorophores Rhodamine B and Rose Bengal agree quite well with the Lorentzian curve (solid line) corresponding to the literature lifetime (3.2 N, 0.9 ns, respectively). In the case of Rose Bengal, that data are observed to be skewed to higher frequencies than the literature lifetime would suggest. In fact, the true lifetime for the solution being employed in these investigations was found by an independent technique to be 0.6 rather than 0.9 ns, because of the presence of an unexpected quencher. This shorter lifetime is in excellent agreement with the recorded data.

To obtain the impulse response function from a fluorophore using a CW laser or other randomly modulated source, a nanosecond correlator must be constructed. Unfortunately, such devices are not commercially available, and must be constructed in the laboratory. To appreciated how such a device might be constructed, let us briefly examine the correlation process itself.

Cross-correlation can be expressed mathematically as

$$C_{1,2}(\tau) = \lim_{T\to\infty} \frac{1}{2T} \int_{-T}^{+T} f_1(t) f_2(t\pm\tau)dt$$

In this expression $f_1(t)$ and $f_2(t)$ are two time-dependent wave forms which are to be correlated, T is the length of each and $C_{1,2}(\tau)$ is the cross-correlation function itself. Because f_2 has a parameter (τ) added to or subtracted from its time position, it has been delayed somewhat with respect to the temporal location

of f_1. To cross-correlate these two wave forms, they must be multiplied, their products integrated over all time, and the result divided by the integration interval. In other words, the product must be time-averaged. This time-averaged product is then displayed in terms of the displacement or delay (τ) between the two wave forms.

Instrumentally, then, one can cross-correlate two time-varying wave forms by delaying one of them, multiplying it by its undelayed partner, and expressing the time average of this product as a function of the delay. Such an instrument is illustrated schematically in Figure 11.

To implement cross-correlation on a nanosecond time scale, both the multiplier and time delay must have nanosecond time response (GHz frequency response) characteristics. A device having these characteristics is illustrated schematically in Figure 12. In Figure 12, fluctuations in the laser are cross-correlated with those in the fluorescence it induces by directing a small fraction of the laser radiation into a fast photodetector (PD_1). The fluctuating photodetector output is then cross-correlated with the output from another fast detector (PD_2) by means of a correlator consisting of a microwave mixer serving as a high-speed multiplier and a time averager constructed from a low-pass electronic filter. Conveniently, the delay between the two signals can be implemented with a movable retroreflector system. Moving the reflector lengthens the path between laser and PD_1, so the radiation arrives at the detector a bit later. Knowing the speed of light to be approximately 3 ns/m, one can derive an accurate time scale (3 ps/mm) by measuring the mirror displacement. The resulting cross-correlation (luminescence decay curve) can be traced out on a strip-chart recorder if the retroreflector movement is at constant velocity.

Significantly, instrumentation used to implement this approach is not much more complex than that shown in Figure 12 (16,17). Both CW (16) and mode-locked (17) lasers have been employed in this kind of application and both have yielded high-quality time-resolved decay curves. A range of fluorophores were investigated and life-time resolution down to 10 ps has already been obtained, using deconvolution procedures. A similar approach, but using auto-correlation and an electronic rather than optical delay line has been applied to the measurement of picosecond laser pulses (18).

Clearly, these new correlation-based approaches to luminescence lifetime measurements offer exciting alternatives to conventional techniques. No matter whether the frequency response or impulse response functions are measured, the perturbing radiation can be applied to the sample over extended periods of time, rather than in a single pulse. Also, when implemented using laser mode noise, no exotic mode-locking laser accessories are required. Finally, the instruments are inherently simple and inexpensive to construct and possess an inherently high degree of temporal resolution.

However, the methods exhibit several drawbacks as well. Unlike the time-correlated single-photon technique, entire detector response times enter into the measured luminescence curves, requiring extensive deconvolution (the time-correlated single photon technique is limited in time resolution by the photodetector's leading edge uncertainty rather than by its pulse width). Also, they inherently require a higher light flux than the single-photon method, a situation which can lead to sample photodecomposition. However, the high speed signal processing which these new methods permit and their other advantages urge that investigation into their use be continued and that they be applied to new fluorescent systems to explore their range of applicability.

Figure 1. Schematic illustration of the concept of a system transfer function. P(t) - Time-dependent input perturbation; T = transfer function of the system (T is a function of system properties A, B,....); R(t) = response of the system as a function of time (R is a function of the perturbation, P, and the transfer function, T).

Figure 2. (a) Schematic illustation of the measurement of a system's response at frequency f. P_0 = amplitude of the sinusoidal input; R_0 = amplitude of the resulting sinusoidal output; ϕ = phase lag of the response, R(t), relative to the input perturbation, P(t). (b) The system's frequency response function.. $A(f) = \frac{R_0}{P_0}$ = amplitude of the system's response relative to the input perturbation as a function of frequency = amplitude portion of the frequency response function; $\phi(f)$ = phase shift of the system's response relative to the input perturbation as a function of frequency = phase portion of the frequency response function.

Figure 3. Schematic illustration of the measurement of a system's impulse response function. P(t) and R(t) are the particular time-dependent input and output functions to the system being perturbed. $\delta(t)$ = delta function input; I(t) = the system's impulse response function.

Figure 4. Schematic illustration of the convolution process. P(t) - amplitude-time profile of the input signal; R(t) = response of the system as a function of time; I(t) = impulse response function of the system. See text for explanation.

Figure 5. Generation of an impulse response function using a noisy perturbing source. Top: autocorrelation of a random waveform produces a delta function. $C_{1,1}(\tau)$ = autocorrelation function. τ = autocorrelation displacement. Bottom: cross correlation of a random perturbation with the response it elicits to generate the impulse response function. $C_{1,2(\tau)}$ = cross-correlation function.

Figure 6. Illustration of the amplitude, A(f), and phase, $\phi(f)$, of the Lorentzian frequency response function of a fluorophore with excited-state lifetime τ.

Figure 7. Hypothetical instrument for measuring luminescence lifetimes using a randomly modulated light source.

Figure 8. Obtaining luminescence lifetimes using a CW laser as a multifrequency modulated light source. Top plot illustrates laser mode beats, which occur at discrete frequencies = c/2L (c = speed of light; L = laser cavity length). Bottom plot illustrates attenuation of mode beats at high frequencies which is caused by finite lifetime of fluorophore. See text for discussion.

Figure 9. Mode beat plots obtained with the instrument shown in Figure 8. A. Mode beats in laser, measured with a scattering suspension in the sample curvette. B. Fluorescence beat plot obtained from Rhodamine B. C. Plot corresponding to

Rose Bengal. Reproduced with permission from reference 14.

Figure 10. Normalized Lorentzian frequency-response curves of two fluorophores, obtained from the data shown in Figure 9. Open circles denote data points; solid lines represent Lorentzian curves fit to the literature lifetime for each fluorophore (given as τ values). Reproduced with permission from reference 14.

Figure 11. Schematic diagram of a cross correlator. See text for discussion.

Figure 12. Instrument for obtaining luminescence lifetimes using a time-varying laser source and an optical cross correlator. PM = photomultiplier tube; BS = beam splitter; C = sample cuvette; M = mirrors or reflectors; PD = high-speed photodiode, A = amplifier; R, L, I = Reference (R) and Local oscillator (L) inputs and Intermediate-frequency (I) output of a double-balanced microwave mixer serving as a multiplier.

REFERENCES

1. G. G. Stokes, Phil. Trans. Roy. Soc. London 142, 463 (1852).
2. E. Gaviola, Z. Physik 35, 748 (1926).
3. G. Horlick and G. M. Hieftje, "Correlation Methods in Chemical Data Measurement", ch. 3 in Contemporary Topics in Analytical and Clinical Chemistry, D. M. Hercules, G. M. Hieftje, L. R. Snyder, M. A. Evanson, eds., Plenum Press, N.Y., 1978, vol. 3.
4. D. Magde, E. Elson, and W. W. Webb, Phys. Rev. Lett. 29, 705 (1972).
5. Y. Chen, J. Chem. Phys. 59, 5810 (1973).
6. B. J. Berne and R. Pecora, Ann. Rev. Phys. Chem. 25, 233 (1974).
7. B. R. Ware and W. H. Flygare, Chem. Phys. Lett. 12, 81 (1971).
8. W. R. Ware, "Transient Luminescence Measurements", ch. 5 in Creation and Detection of the Excited State, A. A. Lamola, ed., Marcel Dekker, N.Y., 1971, vol. 1A.
9. M. A. West and G. S. Beddard, Amer. Lab, Nov., 1976, p. 77.
10. K. G. Spears, L. E. Cramer, and L. D. Hoffland, Rev. Sci. Instrum. 49, 255 (1978).
11. R. D. Spencer and G. Weber, Ann. N.Y. Acad. Sci. 158, 361 (1969).
12. E. R. Menzel and Z. D. Popovic, Rev. Sci. Instrum. 49, 39 (1978).
13. A. E. W. Knight and B. K. Selinger, Spectrochim. Acta, Part A 27, 1223 (1971).
14. G. M. Hieftje, G. R. Haugen, and J. M. Ramsey, Appl. Phys. Lett. 30, 463 (1977).
15. G. M. Hieftje, G. R. Haugen, and J. M. Ramsey, "New Laser-Based Methods for the Measurement of Transient Chemical Events", in New Applications of Lasers to Chemistry, G. M. Hieftje, ed., ACS Symposium Series no. 85, American Chemical Society, Washington, D.C., 1978.

16. C. C. Dorsey, J. M. Pelletier, and J. M. Harris, Rev. Sci. Instrum. 50, 333 (1979).

17. J. M. Ramsey, G. M. Hieftje, and G. R. Haugen, Appl. Optics 18, 1913 (1979).

18. J. M. Ramsey, G. M. Hieftje, and G. R. Haugen, Rev. Sci. Instrum. 50, 997 (1979).

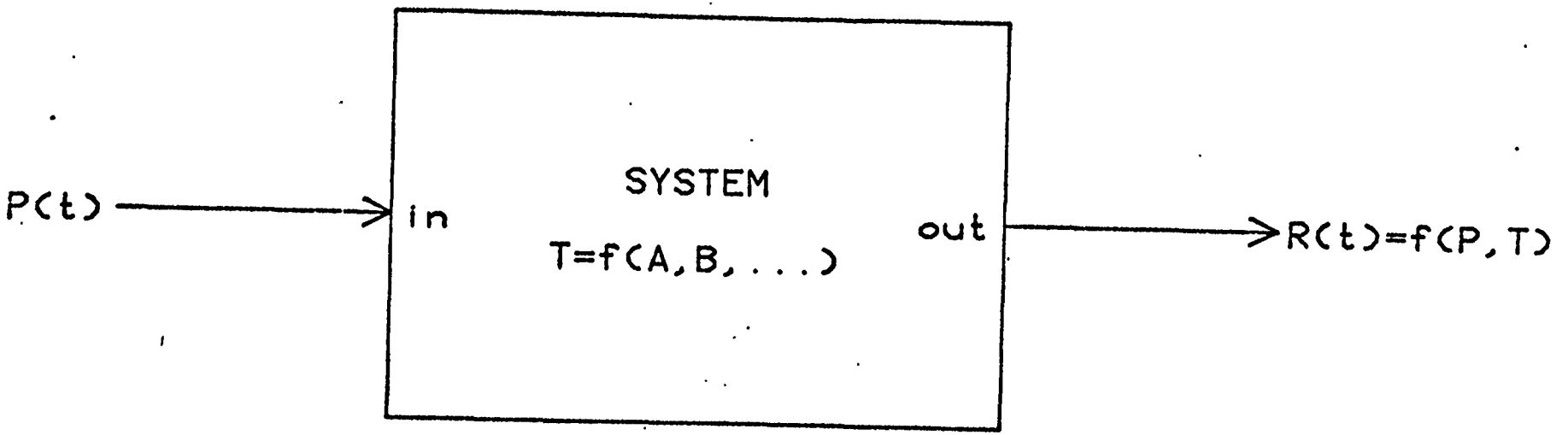
P(t)
in
SYSTEM
T=f(A, B, . . .)
out
R(t)=f(P, T)

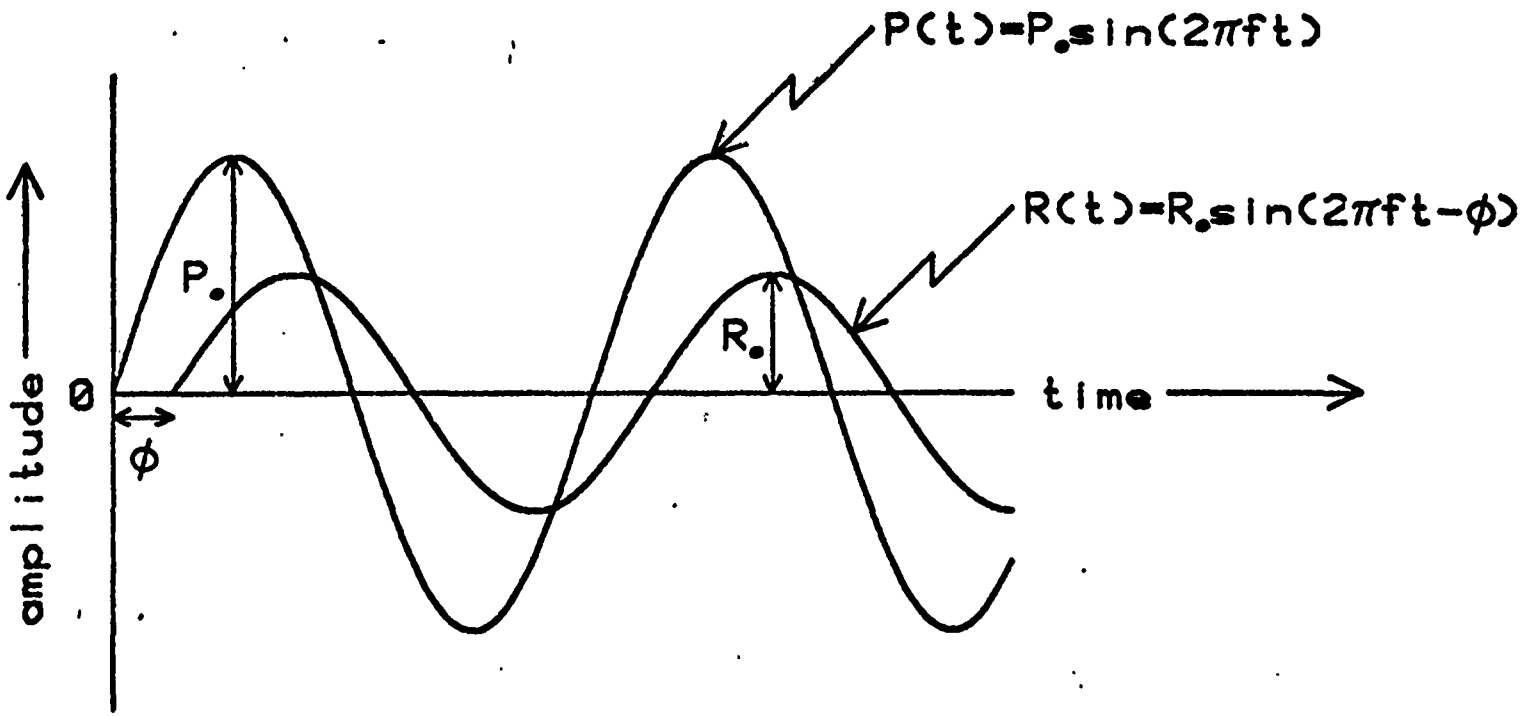

(a)

Fig 2a

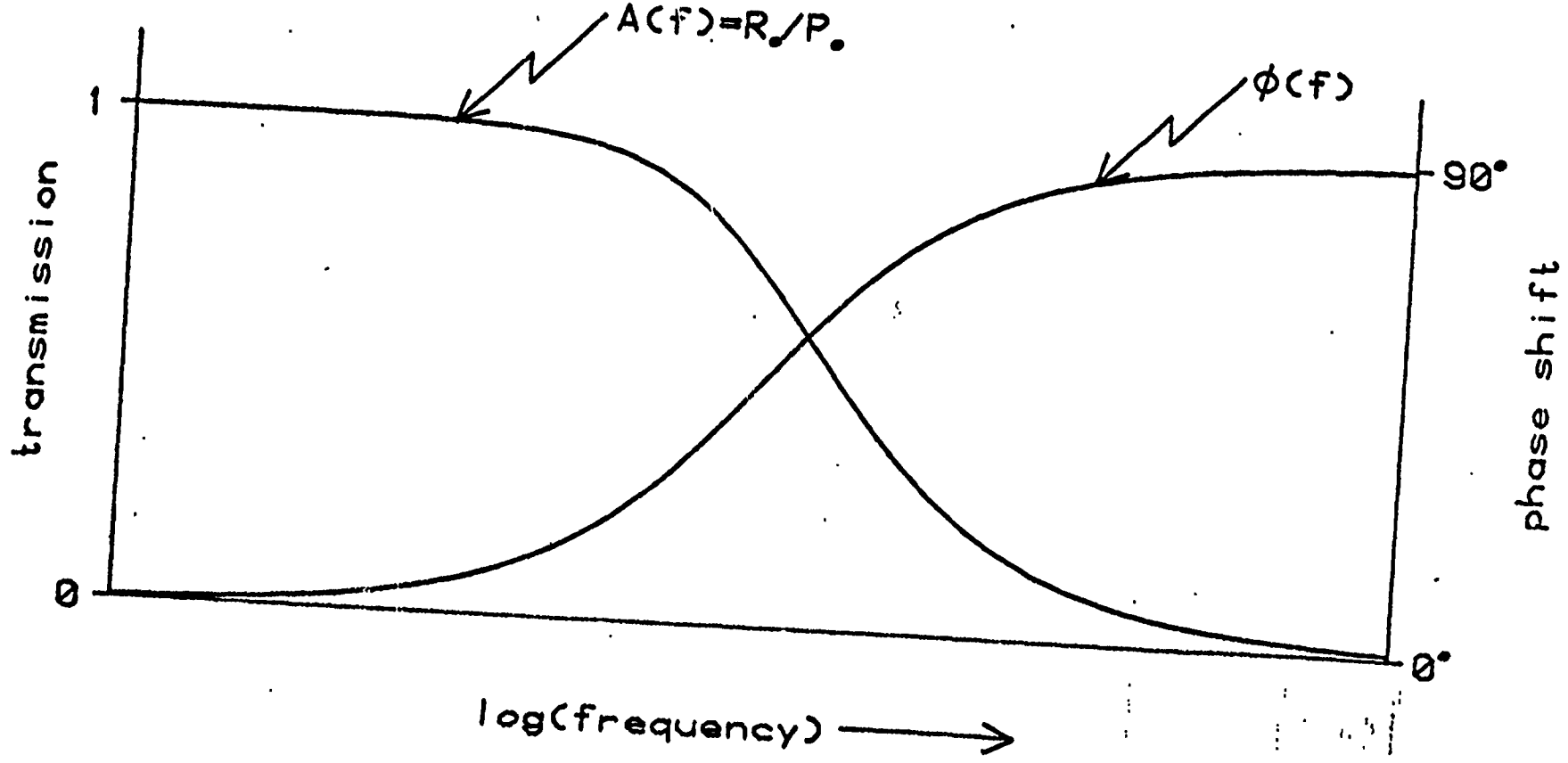

(b)

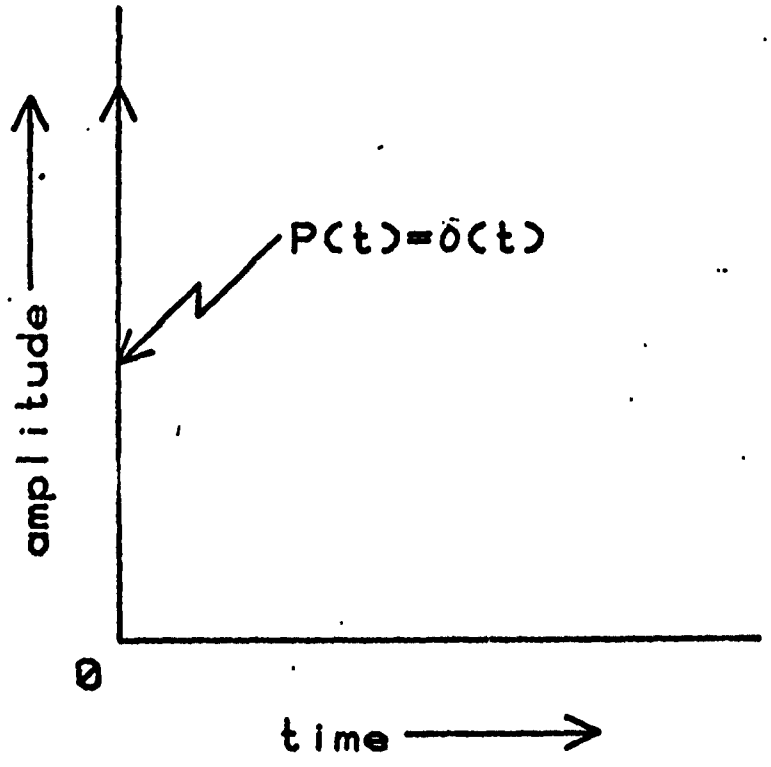

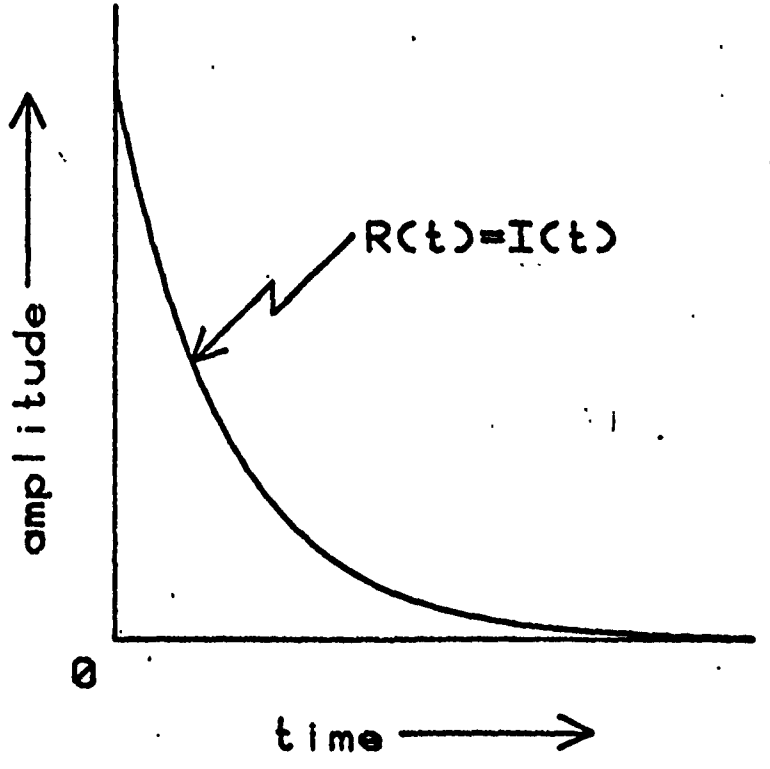

Fig 3

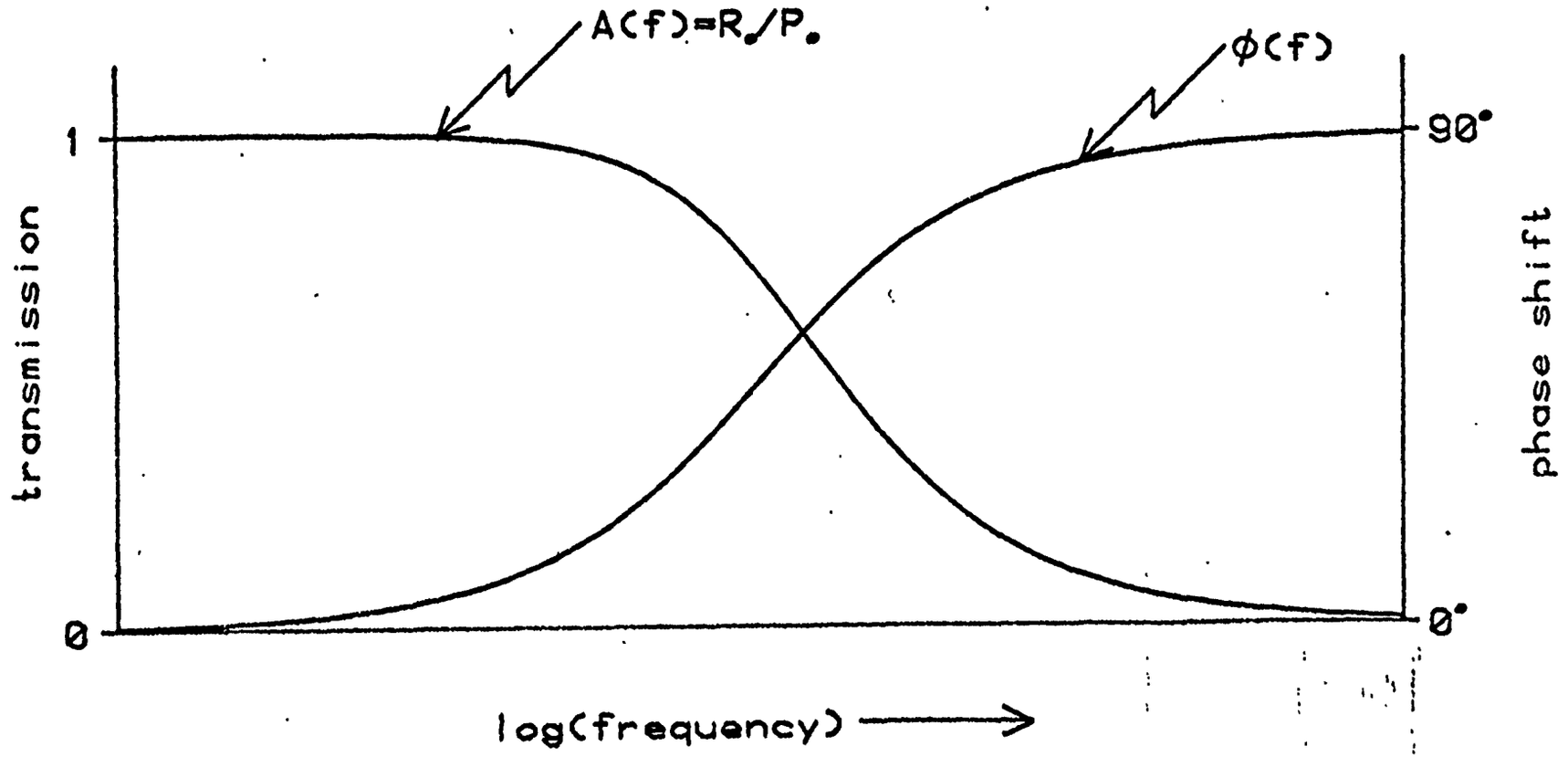

(b)

Fig 2b

R(t)=I(t)
amplitude
time
0

P(t)=δ(t)
amplitude
time
0

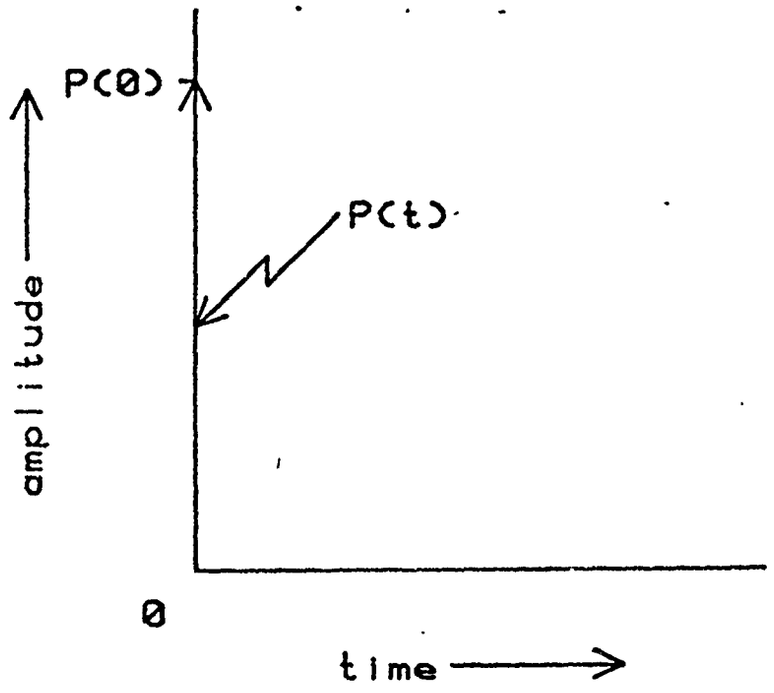

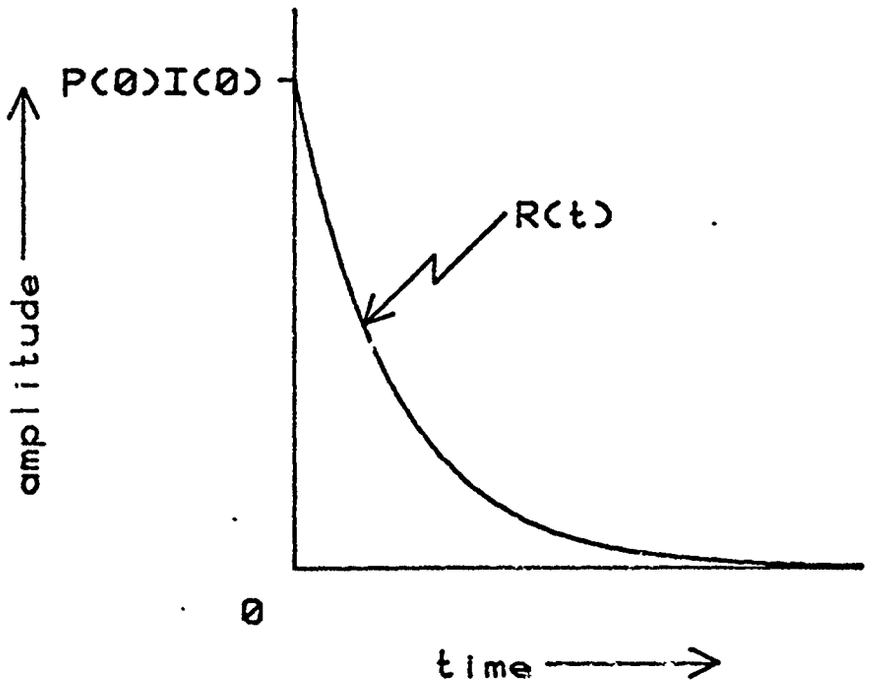

(a)

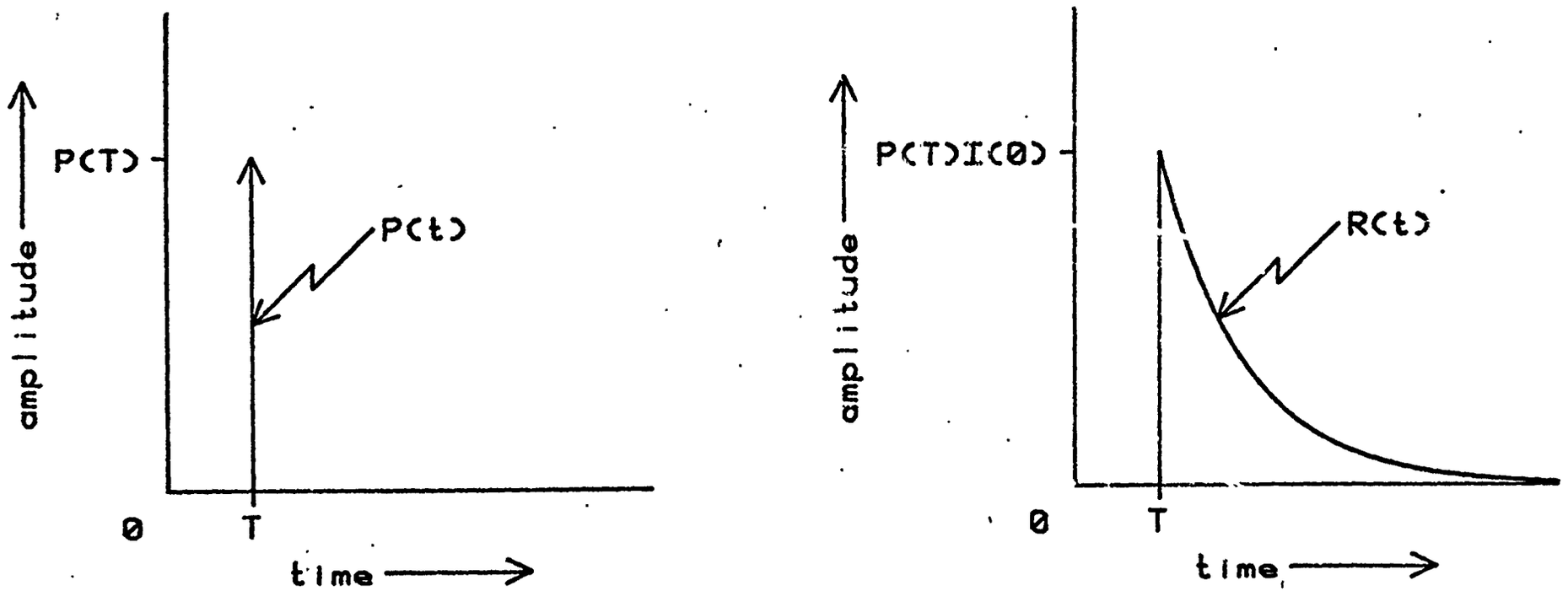

(b)

Fig. 4b

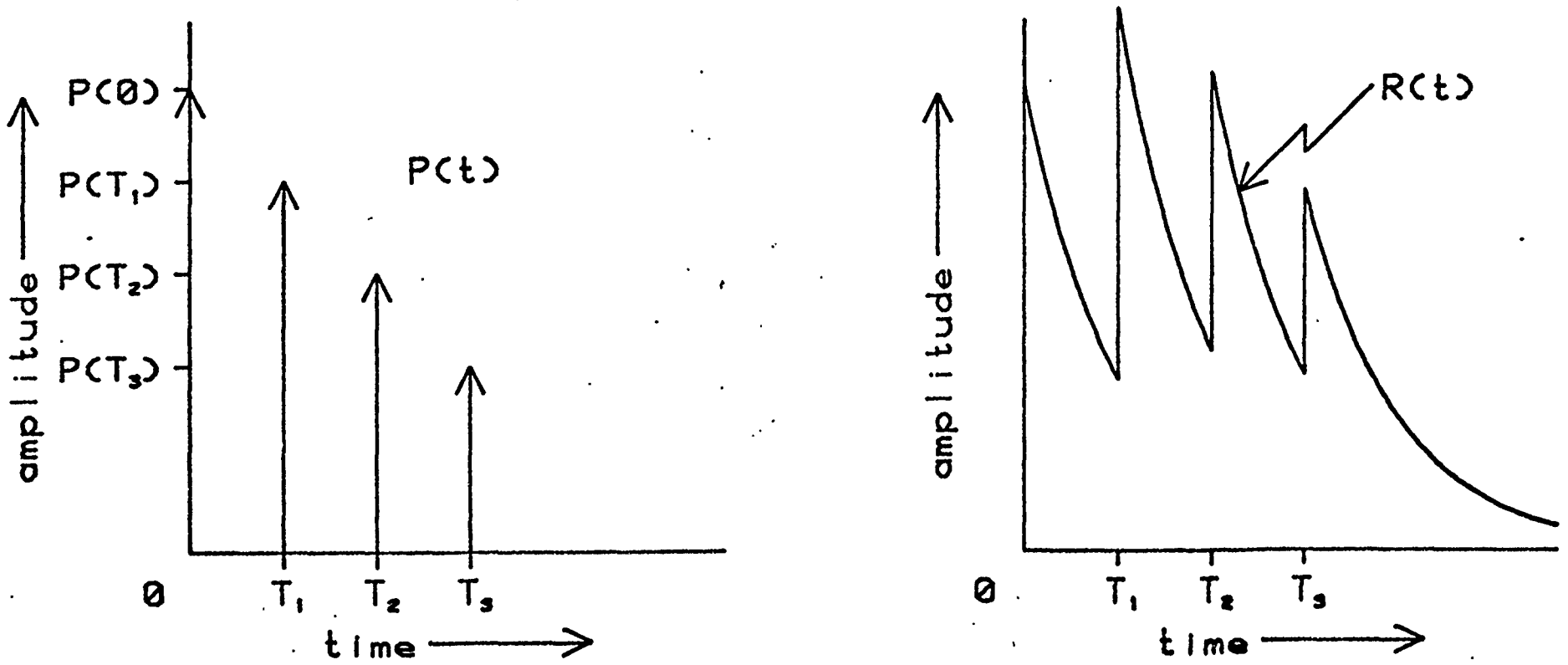
P(0)
P(T1)
P(T2)
P(T3)
P(t)
amplitude
0
T1
T2
T3
time
R(t)
amplitude
0
T1
T2
T3
time

(c)

Fig. 4.c

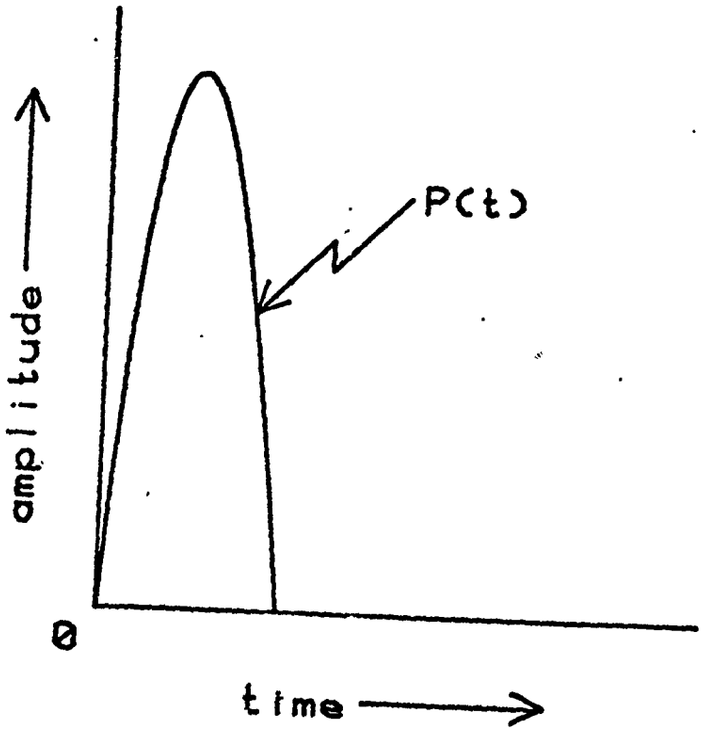

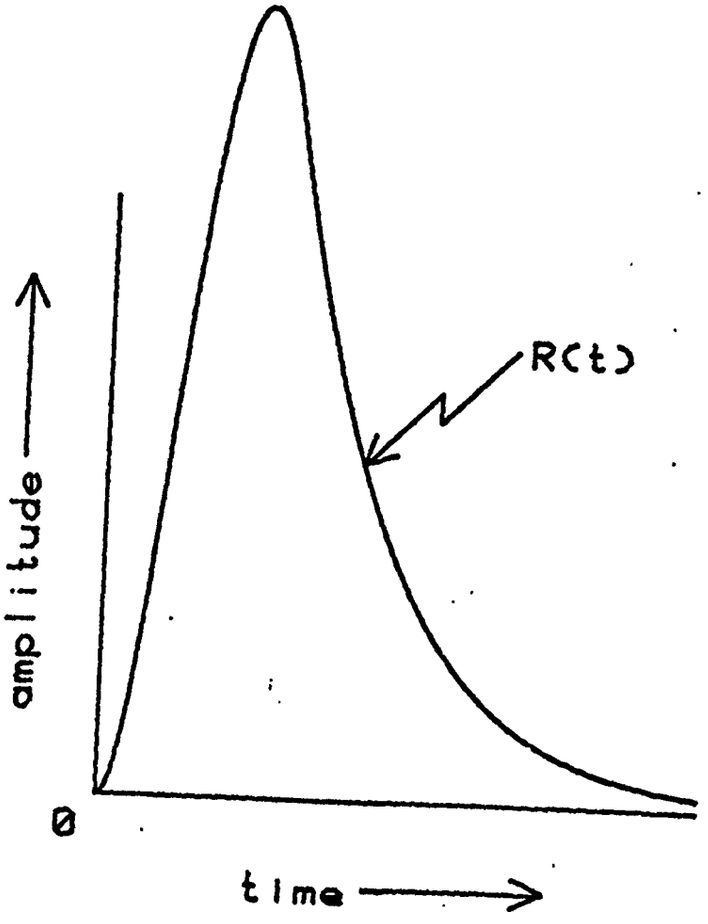

(d)

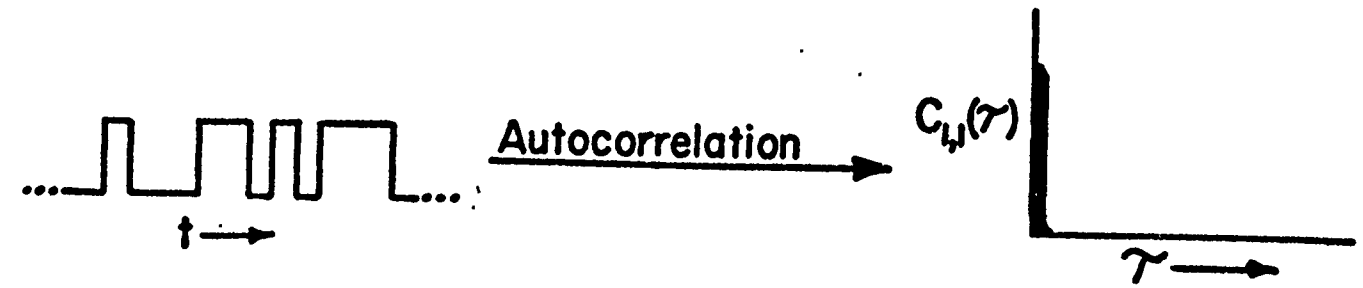
Autocorrelation
$C_{1,1}(\tau)$
t
τ

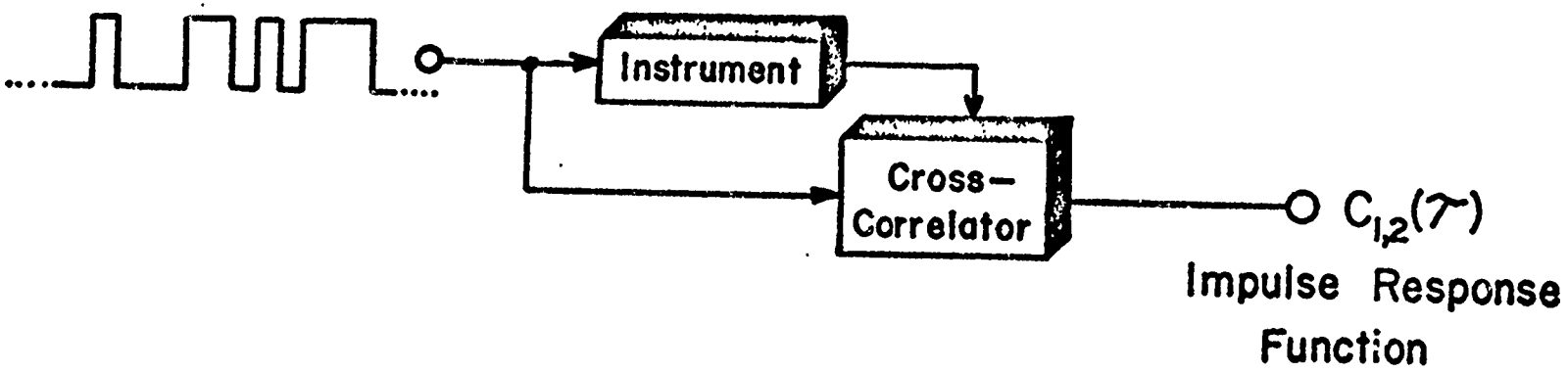
Instrument
Cross–
Correlator
$C_{1,2}(\tau)$
Impulse Response
Function

Fig. 5

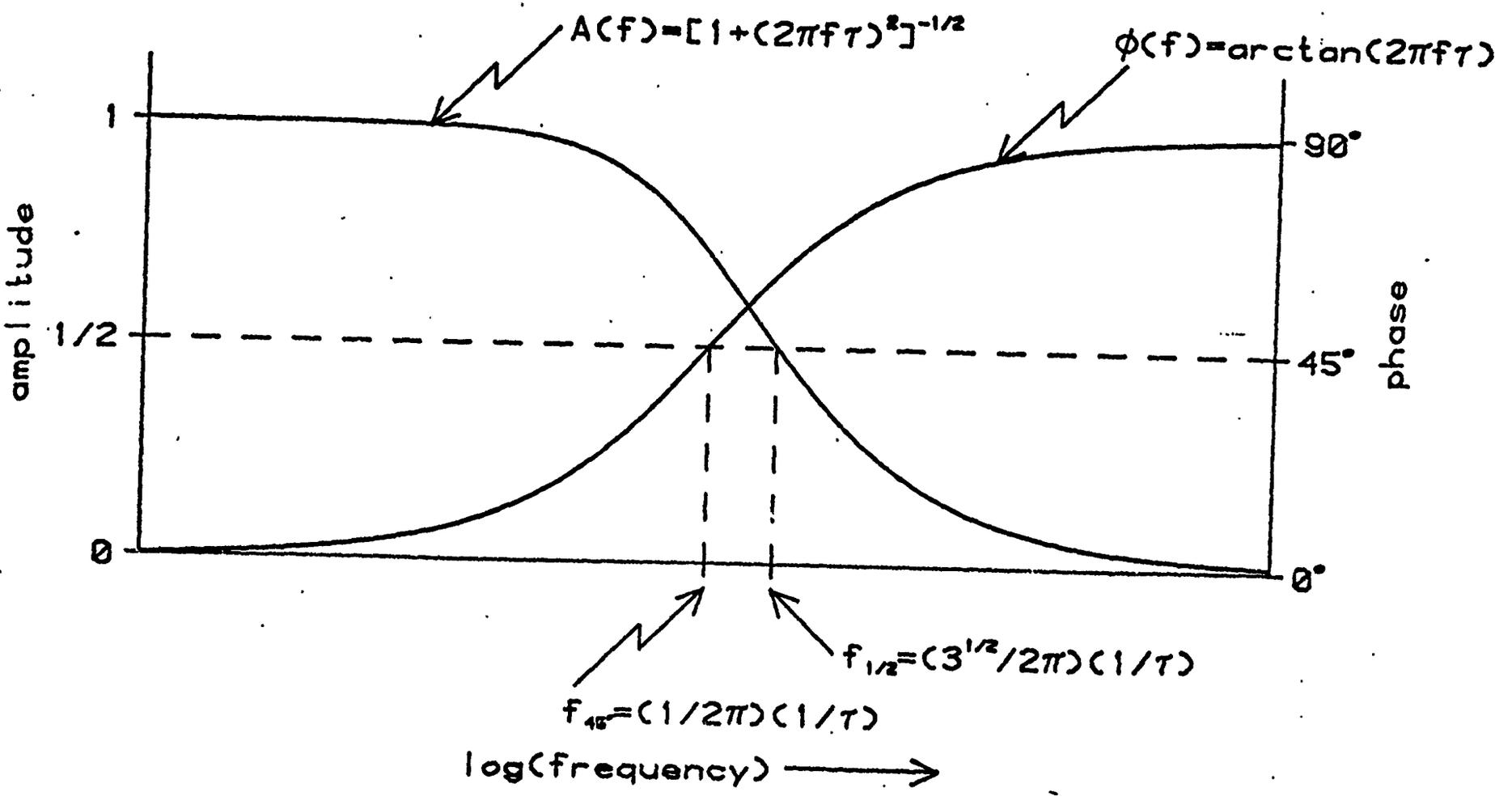
A(f)=[1+(2πfτ)²]^-1/2
φ(f)=arctan(2πfτ)
1
1/2
0
amplitude
90°
45°
0°
phase
f1/2=(3^1/2/2π)(1/τ)
f45°=(1/2π)(1/τ)
log(frequency) ⟶

Fig. 6

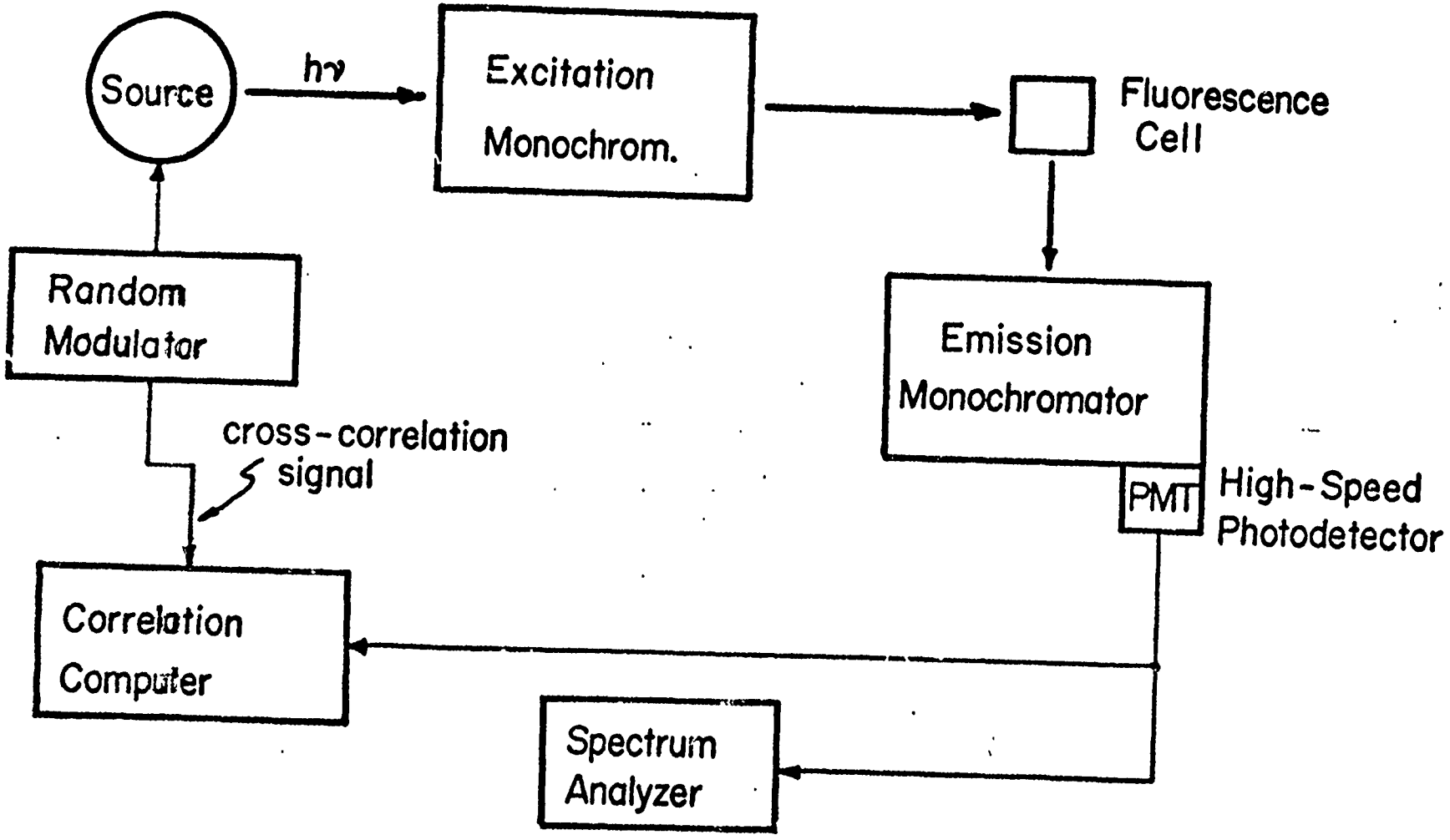
Source
hν
Excitation
Monochrom.
Fluorescence
Cell
Random
Modulator
Emission
Monochromator
cross-correlation
signal
PMT
High-Speed
Photodetector
Correlation
Computer
Spectrum
Analyzer

Fig 7

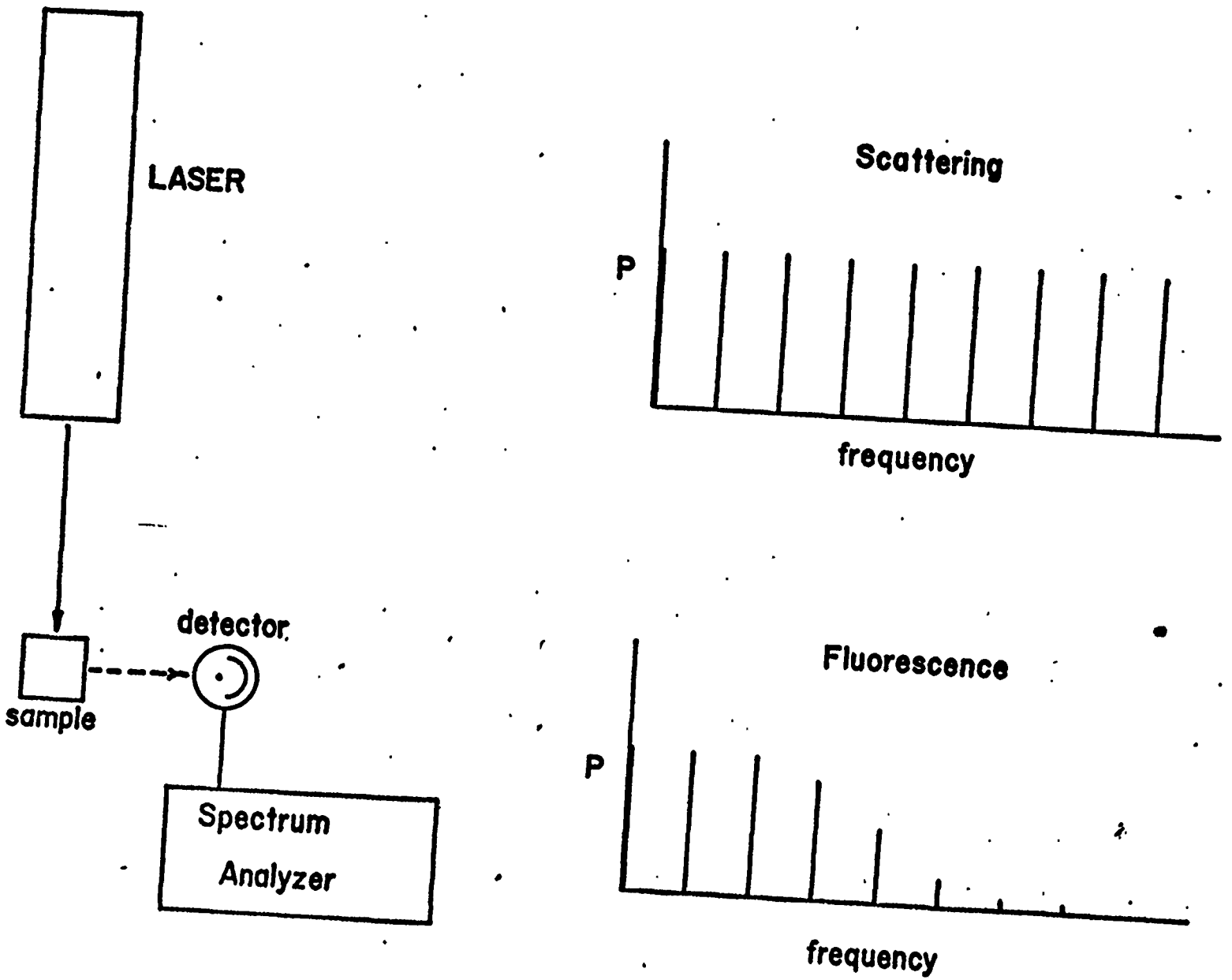
LASER
sample
detector
Spectrum
Analyzer
Scattering
P
frequency
Fluorescence
P
frequency

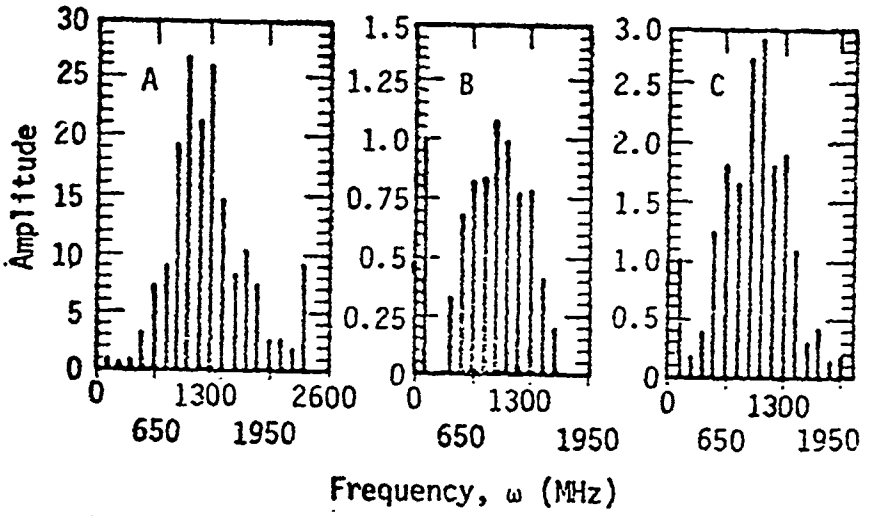
Amplitude
A
B
C
30
25
20
15
10
5
0
1.5
1.25
1.0
0.75
0.5
0.25
0
3.0
2.5
2.0
1.5
1.0
0.5
0
1300
2600
650
1950
Frequency, ω (MHz)

Fig 9

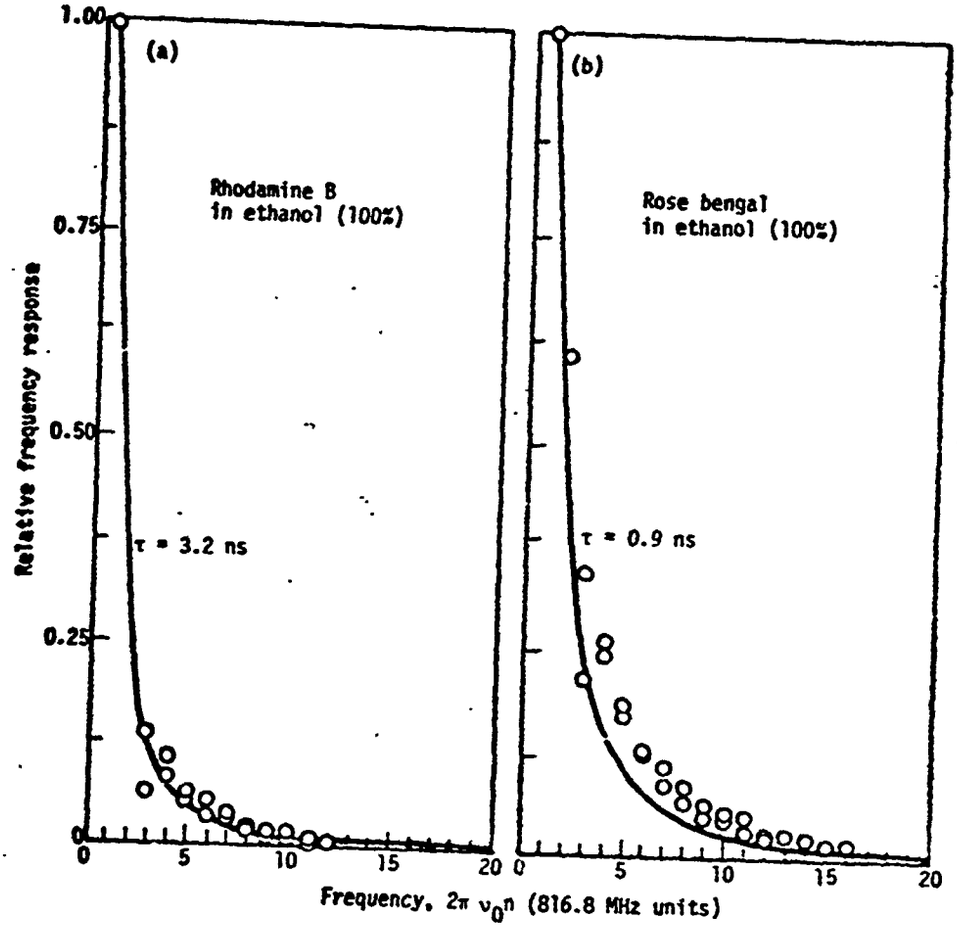
1.00
0.75
0.50
0.25
0
(a)
Rhodamine B
in ethanol (100%)
τ = 3.2 ns
(b)
Rose bengal
in ethanol (100%)
τ = 0.9 ns
Relative frequency response
0
5
10
15
20
Frequency, 2π ν0n (816.8 MHz units)

Fig. 10

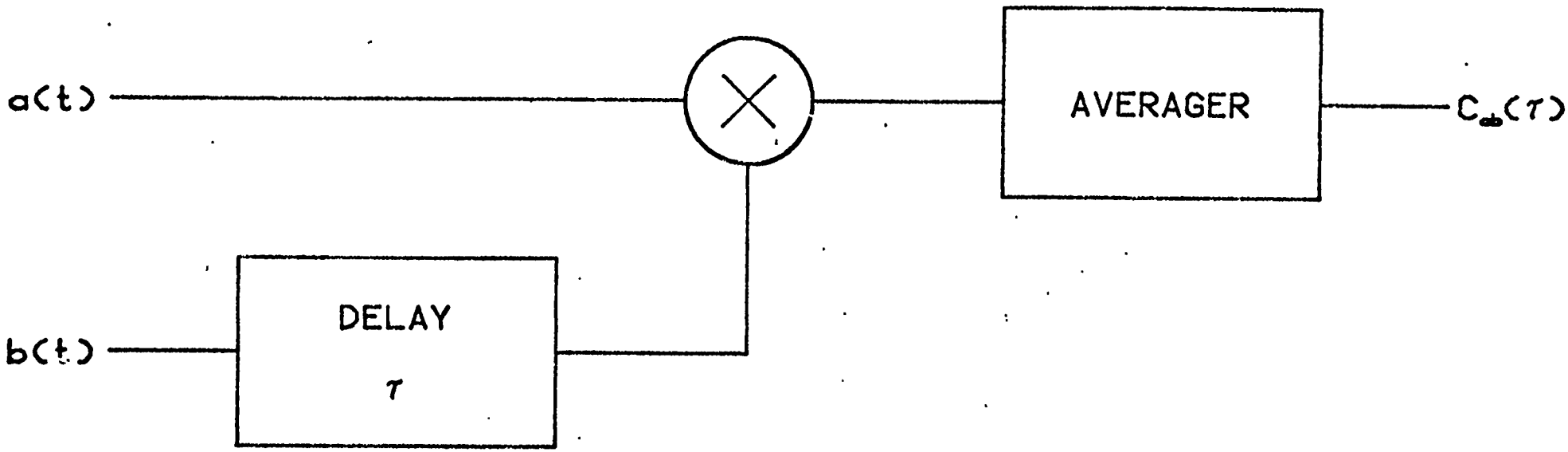

Fig 11

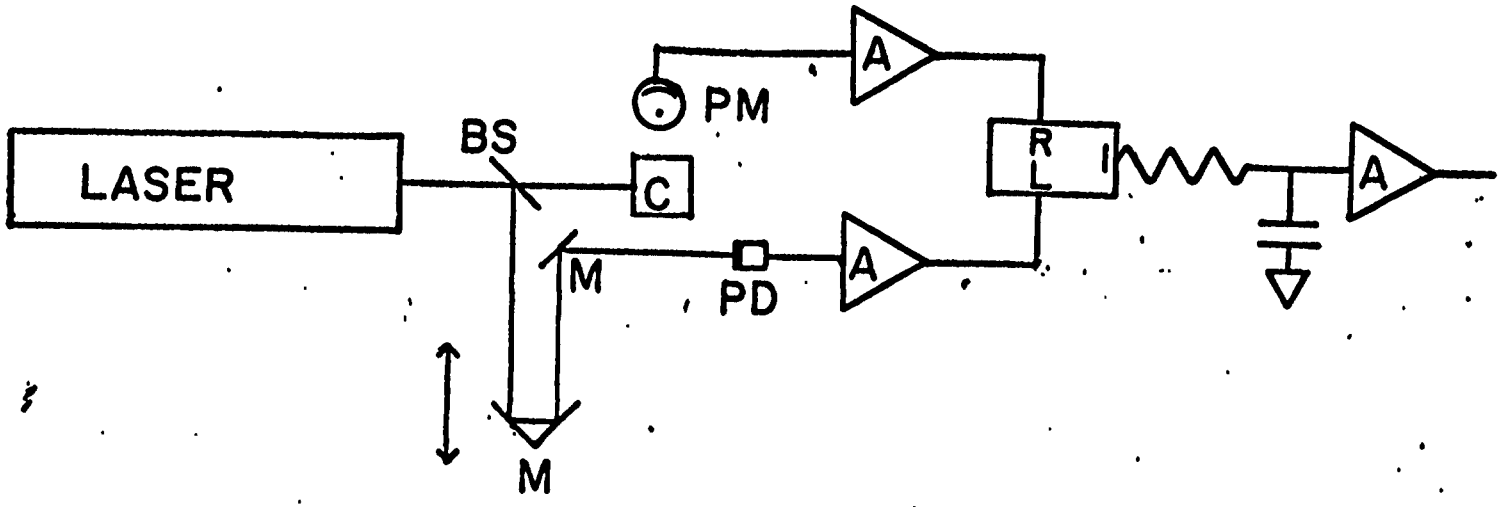

Fig. 12

P4-2/B13

472:GAN:716:1a
78u472-608

TECHNICAL REPORT DISTRIBUTION LIST, 051C

	No. Copies
Dr. M. B. Denton Department of Chemistry University of Arizona Tucson, Arizona 85721	1
Dr. R. A. Osteryoung Department of Chemistry State University of New York at Buffalo Buffalo, New York 14214	1
Dr. B. R. Kowalski Department of Chemistry University of Washington Seattle, Washington 98105	1
Dr. S. P. Perone Department of Chemistry Purdue University Lafayette, Indiana 47907	1
Dr. D. L. Venezky Naval Research Laboratory Code 6130 Washington, D.C. 20375	1
Dr. H. Freiser Department of Chemistry University of Arizona Tuscon, Arizona 85721	
Dr. Fred Saalfeld Naval Research Laboratory Code 6110 Washington, D.C. 20375	1
Dr. H. Chernoff Department of Mathematics Massachusetts Institute of Technology Cambridge, Massachusetts 02139	1
Dr. K. Wilson Department of Chemistry University of California, San Diego La Jolla, California	1
Dr. A. Zirino Naval Undersea Center San Diego, California 92132	1

	No. Copies
Dr. John Duffin United States Naval Postgraduate School Monterey, California 93940	1
Dr. G. M. Hieftje Department of Chemistry Indiana University Bloomington, Indiana 47401	1
Dr. Victor L. Rehn Naval Weapons Center Code 3813 China Lake, California 93555	1
Dr. Christie G. Enke Michigan State University Department of Chemistry East Lansing, Michigan 48824	1
Dr. Kent Eisentraut, MST Air Force Materials Laboratory Wright-Patterson AFB, Ohio 45433	1
Walter G. Cox, Code 3632 Naval Underwater Systems Center Building 148 Newport, Rhode Island 02840	1
Dr. Rudolph J. Marcus Office of Naval Research Scientific Liaison Group American Embassy APO San Francisco 96503	
Mr. James Kelley DTNSRDC Code 2803 Annapolis, Maryland 21402	

P4-2/A23

472:GAN:716:tam
78u472-608

TECHNICAL REPORT DISTRIBUTION LIST, GEN

	No. Copies
Office of Naval Research Attn: Code 472 800 North Quincy Street Arlington, Virginia 22217	2
ONR Branch Office Attn: Dr. George Sandoz 536 S. Clark Street Chicago, Illinois 60605	1
ONR Branch Office Attn: Scientific Dept. 715 Broadway New York, New York 10003	1
ONR Branch Office 1030 East Green Street Pasadena, California 91106	1
ONR Branch Office Attn: Dr. L. H. Peebles Building 114, Section D 666 Summer Street Boston, Massachusetts 02210	1
Director, Naval Research Laboratory Attn: Code 6100 Washington, D.C. 20390	1
The Assistant Secretary of the Navy (R,E&S) Department of the Navy Room 4E736, Pentagon Washington, D.C. 20350	1
Commander, Naval Air Systems Command Attn: Code 310C (H. Rosenwasser) Department of the Navy Washington, D.C. 20360	1
Defense Documentation Center Building 5, Cameron Station Alexandria, Virginia 22314	12
Dr. Fred Saalfeld Chemistry Division Naval Research Laboratory Washington, D.C. 20375	1
U.S. Army Research Office Attn: CRD-AA-IP P.O. Box 1211 Research Triangle Park, N.C. 27709	1
Naval Ocean Systems Center Attn: Mr. Joe McCartney San Diego, California 92152	1
Naval Weapons Center Attn: Dr. A. B. Amster, Chemistry Division China Lake, California 93555	1
Naval Civil Engineering Laboratory Attn: Dr. R. W. Drisko Port Hueneme, California 93401	1
Department of Physics & Chemistry Naval Postgraduate School Monterey, California 93940	1
Dr. A. L. Slafkosky Scientific Advisor Commandant of the Marine Corps (Code RD-1) Washington, D.C. 20380	1
Office of Naval Research Attn: Dr. Richard S. Miller 800 N. Quincy Street Arlington, Virginia 22217	1
Naval Ship Research and Development Center Attn: Dr. G. Bosmajian, Applied Chemistry Division Annapolis, Maryland 21401	1
Naval Ocean Systems Center Attn: Dr. S. Yamamoto, Marine Sciences Division San Diego, California 91232	1
Mr. John Boyle Materials Branch Naval Ship Engineering Center Philadelphia, Pennsylvania 19112	1